5980–5994 *Nucleic Acids Research, 2017, Vol. 45, No. 10* *Published online 27 April 2017*
doi: 10.1093/nar/gkx296

Downstream element determines RNase Y cleavage of the *saePQRS* operon in *Staphylococcus aureus*

Gabriella Marincola and Christiane Wolz*

Interfaculty Institute of Microbiology and Infection Medicine, University of Tübingen, Tübingen 72076, Germany

Received September 02, 2016; Revised March 27, 2017; Editorial Decision April 08, 2017; Accepted April 12, 2017

ABSTRACT

In gram-positive bacteria, RNase J1, RNase J2 and RNase Y are thought to be major contributors to mRNA degradation and maturation. In *Staphylococcus aureus*, RNase Y activity is restricted to regulating the mRNA decay of only certain transcripts. Here the *saePQRS* operon was used as a model to analyze RNase Y specificity in living cells. A RNase Y cleavage site is located in an intergenic region between *sae*P and *saeQ*. This cleavage resulted in rapid degradation of the upstream fragment and stabilization of the downstream fragment. Thereby, the expression ratio of the different components of the operon was shifted towards *saeRS*, emphasizing the regulatory role of RNase Y activity. To assess cleavage specificity different regions surrounding the *sae* CS were cloned upstream of truncated *gfp*, and processing was analyzed *in vivo* using probes up- and downstream of CS. RNase Y cleavage was not determined by the cleavage site sequence. Instead a 24-bp double-stranded recognition structure was identified that was required to initiate cleavage 6 nt upstream. The results indicate that RNase Y activity is determined by secondary structure recognition determinants, which guide cleavage from a distance.

INTRODUCTION

RNA decay is a crucial process for coordinating prokaryotic gene expression. In gram-positive bacteria, RNase J1, RNase J2 and RNase Y are thought to be major contributors to mRNA degradation and maturation (1–6). Two different models of RNA decay have been described: RNA decay can be triggered by pyrophosphohydrolase (RppH), which removes the pyrophosphate from the 5′ end of triphosphorylated RNA transcripts. The monophosphorylated RNA can then be processed via the exoribonuclease activity of RNase J1 (7). Degradation can also be initiated via the so-called direct entry pathway, starting with endonucleolytic cleavage. RNA decay continues via the 5′ to 3′ exoribonuclease activity of RNase J1 and the 3′ to 5′ exoribonuclease activity of PNPase. Initiation by endolytic cleavage is likely to be the major pathway of mRNA decay. For *Bacillus subtilis*, RNase Y has been proposed to be the enzyme responsible for endonucleolytic cleavage of bulk mRNAs (8–10) and thus the functional equivalent of *Escherichia coli* RNase E.

Analyses of RNase Y function in *Staphylococcus aureus* revealed that, at least in this organism, RNase Y activity is kept under tight control (11,12). RNase Y mutants in *S. aureus* are only slightly impaired in growth and only ∼100 cleavage sites were identified using whole-genome analysis (12). However, RNase Y has been shown to be required for virulence gene expression at the promoter level (11) and *rny* deletion mutants exhibit reduced virulence (11,13). To date, it is largely unclear how the activation of virulence genes is mediated by RNase Y. Several non-coding RNAs and the primary transcript of the regulatory *saePQRS* operon were found to be processed by RNase Y (11,12). RNase Y-mediated processing of these RNA species is probably important for the coordinated expression of virulence genes.

The *saePQRS* operon encodes four different proteins. SaeR and SaeS are part of a bacterial two-component system with a response regulator and a histidine kinase that control the expression of major virulence genes in *S. aureus* (14–16). The functions of SaeP and SaeQ are not clear. It has been suggested that these two proteins assist the activated Sae system to return to its pre-stimulus state (17–19). The *sae* operon (Figure 1A) is transcribed from two promoters (P1 and P3) and a total of four overlapping RNAs (T1–T4) are detectable. The mature T1 transcript is transcribed from the major auto-activated P1 promoter. The most abundant and stable T2 RNA is generated by RNase Y-dependent endoribonucleolytic cleavage of T1 (11,20). T3 is transcribed from the constitutive P3 promoter to ensure a basal level of *saeRS* expression. T4 is also initiated at the P1 promoter but encompasses a monocistronic RNA encoding only *saeP*. T4 may be either a processed product of T1 or a prematurely terminated *de novo* transcript from P1 (14,21).

RNase Y in *B. subtilis* is an integral part of the degradosome, which also contains RNase J1, RNase J2, enolase and the CshA helicase. RNase Y is the only protein in the

*To whom correspondence should be addressed. Tel: +49 7071 298 0187; Fax: +49 7071 295 165; Email: christiane.wolz@med.uni-tuebingen.de
Present address: Gabriella Marincola, Department of Biochemistry, University of Würzburg, Würzburg 97074, Germany.

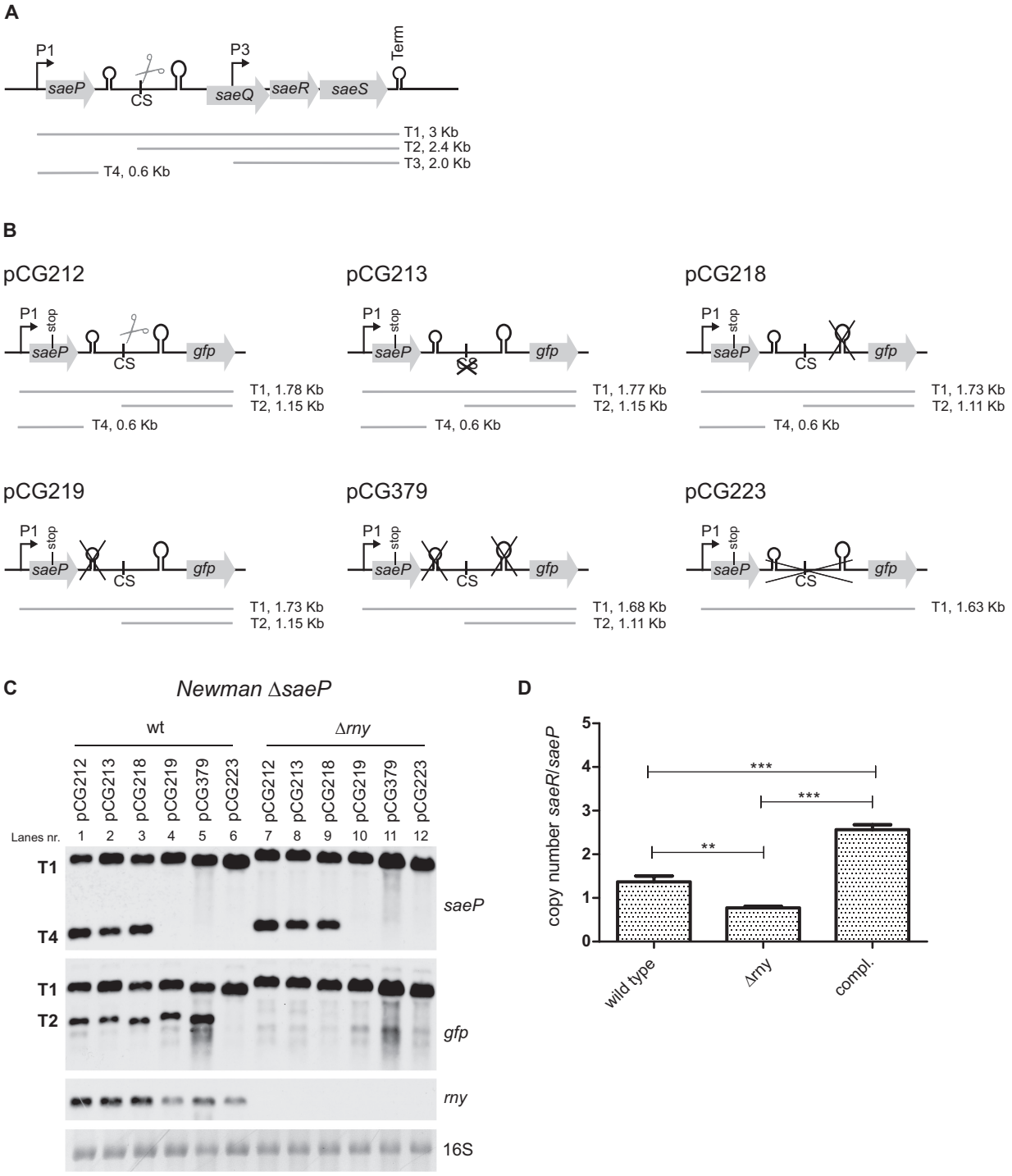

Figure 1. RNase Y allows differential expression between genes co-expressed in the *saePQRS* operon. (**A**) Schematic representation of the *saePQRS* operon, with its primary and mature RNA molecules (T1–T4), promoters (P1 and P3), terminator (Term), cleavage site (CS) and putative stem loops. (**B**) Schematic representation of *sae-gfp* constructs carrying different deletions (the deleted sequence is indicated in the panel with a cross). The RNAs observed in the northern blot analyses are indicated with their names and lengths below each constructs. (**C**) Northern blot analyses to examine *sae* processing in strains carrying the *sae-gfp* constructs. Newman *saeP* mutant and *saeP rny* double mutant strains carrying different constructs were grown to exponential phase. RNA was then harvested and hybridized with DIG-labeled DNA probes specific for *gfp*, *saeP* and *rny*. As a loading control, 16S rRNA detected in the ethidium bromide-stained gel was used, which is shown at the bottom of the panel. For clarity, lane numbers are indicated in the panel. (**D**) RT-qPCR to assess the ratio between *saeR* and *saeP* copy numbers. Newman wild-type, *rny* mutant and complemented strains were grown (in triplicate) to late exponential phase and RNA was extracted. After DNase I treatment, one-step RT-qPCR was performed. *saeR* and *saeP* copy numbers were calculated by reference to a standard curve. Statistically significant differences between the samples are indicated: $^{**}P = 0.001$ to 0.01; $^{***}P < 0.001$.

complex with a membrane anchor and is thought to function as a scaffold for the entire machinery (9,22,23). For *B. subtilis*, it has been postulated that an RNase Y membrane anchor is required for function *in vivo* (9). The presence of a degradosome-like complex in *S. aureus* has also been suggested (24). However, the RNase Y of *S. aureus* does not seem to be the key enzyme for complex formation because it does not participate in many protein interactions (24). For RNase Y of *S. aureus,* RNase Y membrane association appears to be required to limit activity and for the further selectivity of RNase Y *in vivo* (12,25).

Our understanding of the structure, enzymatic activity and sequence requirements of RNase Y is still in its infancy. In a recent study, a novel global method called EMOTE (Exact Mapping Of Transcriptome Ends) (26) was used to explore the *in vivo* recognition sequence motif of RNase Y (12). The authors identified a preferred target sequence (a guanosine immediately prior to the cleavage site) (12).

Only a few studies have reported findings for purified RNase Y. RNase Y lacking the N-terminal membrane anchor from *B. subtilis* (8) has been shown to exert endonucleolytic activity of *in vitro*-transcribed 5′ monophosphorylated RNAs. Purified RNase Y from *S. aureus* cleaves the 2′-3′-cyclic phosphodiester linkage at the 3′ terminus (27). The generated 3′ monophosphorylated RNA seems to be protected from PNPase exonucleolytic degradation (28). However, the *in vitro* results are inconsistent with the *in vivo* assays. For example, the preference for 5′ monophoshorylated RNA could not be confirmed *in vivo* (29), and the products generated by RNase Y are readily degraded by PNPase (30). Thus, it appears that the native function of the enzyme cannot be easily mirrored using *in vitro* assays.

The aim of this work was to elucidate the sequence/structural requirements of RNase Y-dependent processes *in vivo*. The *saePQRS* operon was chosen as the model RNA because it contains one of the best defined RNase Y processing sites. At least one cleavage product is stabilized and thus easily detectable (11,12, 20). Here it is shown that in contrast to the downstream fragment, the RNase Y-generated upstream fragment is rapidly degraded. This result implies that RNase Y allows differential expression of genes that are co-expressed from the same operon. Cloning analysis revealed that RNase Y cleavage was not determined by the sequence of the cleavage site. A 24-bp double-stranded recognition structure could be identified that was required to initiate cleavage 6 nt upstream.

MATERIALS AND METHODS

Bacterial strains and growth conditions

The strains used in this study are listed in Table 1. *S. aureus* strains were grown in CYPG medium (10 g l^{-1} casamino acids, 10 g l^{-1} yeast extract, 5 g l^{-1} NaCl, 0.5% w/v glucose and 0.06 M phosphoglycerate) (31). For strains carrying resistance genes, antibiotics were used only in overnight cultures at the following concentrations: 10 μg ml^{-1} erythromycin, 5 μg ml^{-1} tetracycline and 10 μg ml^{-1} chloramphenicol. Bacteria from overnight cultures were diluted to an initial optical density at 600 nm (OD600) of 0.05 in fresh medium and grown with shaking at 220 rpm at 37°C to exponential growth phase.

Plasmid and strain construction

All plasmids and oligonucleotides are listed in Tables 1 and 2, respectively.

saeP deletion mutant and saeP rny double mutant. Replacement of the *saeP* locus with a kanamycin resistance cassette (*kan*) was achieved by overlapping polymerase chain reaction (PCR). The resulting amplicon was digested with KpnI and cloned into pBT2 (32). To take advantage of blue-white selection, the fusion fragments were then subcloned into the EcoRI and SalI sites of pMAD (33). The resulting plasmid, pCWSAE30, was verified and transformed into the restriction-deficient strain RN4220, followed by mutagenesis as described previously (33). The mutant (referred to as RN4220-30) was verified by PCR and pulsed-field gel electrophoresis. The resulting mutation was transduced into Newman, yielding strain Newman-30. The *saeP rny* double mutant (referred to as Newman-217-30) was obtained by transduction of the *rny::ermC* mutation from RN4220-217 (11) into Newman-30.

Construction of sae-gfp fusions. Construction of the integration plasmids was achieved using pCG188 (11), which allows plasmid integration into the *geh* locus. Different deletions in the *sae* region spanning the P1 promoter until upstream of the P3 promoter were introduced by overlapping PCR using oligonucleotides and templates listed in Table 2. The amplicons were ligated into the EcoRI-digested pCG188 to generate the various plasmids listed in Table 1. The correct orientation and sequence of the inserts were verified by PCR using a specific upstream oligonucleotide together with gfp-rev-all, and by Sanger sequencing before integration into the lipase gene of competent *S. aureus* CYL316 (34). The integrated plasmids were subsequently transduced into the appropriate experimental *S. aureus* strains. All transductants were verified by PCR. For cloning of sae-gfp constructs into the replicative plasmid pCG246, the *sae-gfp* region from plasmids pCG212, pCG392, pCG484 and pCG223 was subcloned by Gibson assembly using the oligonucleotides listed in Table 2 to generate pCG599, pCG600, pCG601 and pCG620, respectively. The plasmids were verified by Sanger sequencing, cloned into DC10B and then transferred into electro-competent *S. aureus* strains.

Construction of sae-gfp construct with mutated CS or mutated secondary structure. Point mutations were introduced into selective constructs by site-directed mutagenesis (SDM Q5 Kit, New England Biolabs) according to the manufacturer's instructions using the oligonucleotides listed in Table 2. The CS (C/T) mutation in the *sae* cleavage site was introduced into plasmid pCG212 to generate plasmid pCG589. The *sae-gfp* region in plasmid pCG589 was then subcloned into the replicative plasmid pCG246 by Gibson assembly using the oligonucleotides listed in Table 2 to generate pCG616. Point mutations to prevent secondary structure formation downstream of the CS (Figure 6C) were introduced directly into plasmid pCG599 to generate plasmids pCG618. All plasmids were verified by Sanger sequencing, cloned into DC10B and transferred into electro-competent *S. aureus* strains.

Table 1. Bacterial strains and plasmids

Strain or plasmid	Description	Reference
Strains		
E. coli		
TOP10	Competent *E. coli* for plasmid transformation	Invitrogen
DC10B	Competent *E. coli* for direct plasmid transformation into clinical isolates of *S. aureus*	(46)
BL21 (DE3)	*E. coli* for expression of recombinant proteins with IPTG	Promega
S. aureus		
ISP479C	8325-4 derivative, with $SaeS^{L}$ allele	(47)
CYL316	RN4220(*pYL112Δ19*), L54 *int* gene,	(34)
RN4220	Restriction-deficient *S. aureus* strain	(48)
RN4220-30	RN4220 *saeP::kanA*	This work
RN4220-217	RN4220 *rny*::*ermC*	(11)
Newman	Wild-type	(49)
Newman-29	Newman, *sae::kanA*	(20)
Newman-30	Newman *saeP::kanA*	This study
Newman-217	Newman *rny*::*ermC*	(11)
Newman-217-30	Newman *rny*::*ermC, saeP::kanA*	This work
PR01	*ΔpyrFE* mutant of the clinical strain SA564RD	(39)
PR01-01	PR01 with the RNase J1 gene deleted	(39)
Plasmids		
For SaeP mutant construction		
pMAD	Vector for allelic replacement	(33)
pBT2	Cloning vector	(31)
pCWsae30	pMAD with cloned *saeP::kanA*	This study
For PCR template		
pCWsae19	pCR2.1-Topo with *saePQRS* with stop codon in *saeP*	(T. Geiger, unpublished)
Integrative plasmids		
pCG188	pCL84 with truncated *gfp* gene cassette from pc183	(11)
pCG212	pCG188 with *sae* region from P1 to upstream of P3	(11)
pCG213	pCG188 with *sae* region from P1 to upstream of P3 with deletion of 13 bp in the CS	This work
pCG218	pCG188 with *sae* region from P1 to upstream of P3 with deletion of the left stem loop (terminator)	This work
pCG219	pCG188 with *sae* region from P1 to upstream of P3 with deletion of the right stem loop	This work
pCG223	pCG188 with *sae* region from P1 to upstream of P3 with deletion of the entire region between the two stem loops	This work
pCG379	pCG188 with *sae* region from P1 to upstream of P3 with deletion of the two stem loops	This work
pCG301	pCG188 with *sae* region between the 2 stem loops under the native P1 promoter	This work
pCG392	pCG188 with *sae* region from P1 to upstream of P3 with deletion of the sequence downstream of CS (Rrs)	This work
pCG394	pCG188 with *sae* region from P1 to upstream of P3 with deletion of the CS and alternative CS (aCS)	This work
pCG484	pCG188 with *sae* region from P1 to upstream of P3 with deletion of the Rrs counterpart	This work
pCG589	pCG212 with *sae* region with mutated CS (C instead of T)	This work
Replicative plasmids		
pCG246	*E. coli*/Staphylococcus shuttle vector, pCN47 derivative with *cat* cassette	(50)
pCG599	pCG246 with *sae-gfp* region from plasmid pCG212	This work
pCG600	pCG246 with *sae-gfp* region from plasmid pCG484	This work
pCG601	pCG246 with *sae-gfp* region from plasmid pCG392	This work
pCG616	pCG246 with *sae-gfp* region from plasmid pCG589	This work
pCG618	pCG599 with *sae* region with point mutation which affect Rrs secondary structure: CC in +3 and +8 instead of AA, CC in +14 and +15 instead of TT (the position is indicated as distance to the cleavage site)	This work
pCG620	pCG246 with *sae-gfp* region from plasmid pCG223	This work
For complementation		
pCG296	pCG246 with *rny* for complementation	(11)
pCG322	pCG246 with *rny* without active site for complementation	This work
pCG596	pCG246 with *rny* carrying mutations in the active site (H367A D368A)	This work
For protein purification		
pET15b	Protein expression vector, IPTG inducible	Novagen
pCG249	pET15b with *rny* (without transmembrane domain)	This work

Table 2. Oligonucleotides

Purpose	Template	Name	Sequence
***saeP* deletion mutant**			
	ISP479C	Kpnsae-for	CGGGGTACCATACTACAGTTTTACATT
		Kpn-ORF4-rev	ACCTCGGTACCCTGTTCTTACGACCTCTAAAG
		HybridORF4a-rechts	TAAAAGTTCGCTAGATAGGGGTCCCGCGTATGATTTCACAGCC
		Hybridsae-links	TCCAATTCTCGTTTTCATACCTCGGAGCTAACTCCTCATTTCTTCAATTT
	Newman29	kanR-for	CCGAGGTATGAAAACGAGAATTGG
		kanR-rev	GGGACCCCTATCTAGCGAACTTT
***sae–gfp* fusion in integrative plasmid (pCG188)**			
		Eco-sae-for	GCGTGAATTCTTATTGTGGCAAAAGGTTT
		Eco-sae1283rev	CGTGAATTCTGACGTCGTATGTGCAACTA
		Eco-sae1014rev	GGGAATTCTTATGTGAACAGGAAGTGTTT
control PCRs		gfp-rev-all	GGTATCACCTTCAAACTTGACTT
pCG213	pcwsae19	DelP2for	TCAATATATATACCATAAGATTGC
		DelP2rev	GCAATCTTATGGTATATATATTGA
pCG218	pcwsae19	DelST-orf4for	AGAGCACATAAGAAACACTTCCT
		DelST-orf4rev	AGGAAGTGTTTCTTATGTGCTCT
pCG219	pcwsae19	DelST5for	TCAATGGAAAGCATATATACAACT
		DelST5rev	AGTTGTATATATGCTTTCCATTGA
pCG223	pcwsae19	DelP2longfor	TCAATGGAAAGCAAACACTTCCT
		DelP2longrev	AGGAAGTGTTTGCTTTCCATTGA
pCG379	pCG218	DelST5rev	AGTTGTATATATGCTTTCCATTGA
		DelST5for	TCAATGGAAAGCATATATACAACT
pCG301	pcwsae19	hybridsaePdelrev	CTTTCCATTGAGTAACCTTGATCTTGTGA
		hybridsaePdelfor	CACAAGATCAAGGTTACTCAATGGAAAGC
pCG392	pcwsae19	hybridpCG392rev	TCAAGCTCTAAAAAAATTTAGATTTAATAGTTGTATATAT
		hybridpCG392for	ATATATACAACTATTAAATCTAAATTTTTTTAGAGCTTGAT
pCG394	pcwsae19	hybridpCG394rev	TGTGCTCTGCAATCTTATGGATTGAAAAAAGGAAAGTATG
		hybridpCG394for	CATACTTTCCTTTTTTCAATCCATAAGATTGCAGAGCACA
pCG484	pcwsae19	Hybrid-Rrs-Counter-rev	CGATTTGTAGTGTTATGTGA
		Hybrid-Rrs-Counter-for	TCACATAACACTACAAATCGTTTATATAAATTACACACAAT
pCG589	pCG212	Q5SDMpCG212R	ATATATTGAAAAAAGGAAAGTATGATTTC
		Q5SDMpCG212F	ATACAACTATCAAATCCCATAAGATTG
***sae–gfp* fusion in replicative plasmid (pCG246)**			
pCG599	pCG212	Gibson-saeconstr-for	ATTTAGAATAGGCGCGCCTGAATTCTTATTGTGGCAAAAGGTTTATAA ATTTTAATAC
		Gibson-saeconstr-rev	ATCCCCGGGTACCGAGCTCGAATTCTTACAAACAAAAAGCGGATTAC
pCG600	pCG484	Gibson-saeconstr-for	ATTTAGAATAGGCGCGCCTGAATTCTTATTGTGGCAAAAGGTTTATAA ATTTTAATAC
		Gibson-saeconstr-rev	ATCCCCGGGTACCGAGCTCGAATTCTTACAAACAAAAAGCGGATTAC
pCG601	pCG392	Gibson-saeconstr-for	ATTTAGAATAGGCGCGCCTGAATTCTTATTGTGGCAAAAGGTTTATAA ATTTTAATAC
		Gibson-saeconstr-rev	ATCCCCGGGTACCGAGCTCGAATTCTTACAAACAAAAAGCGGATTAC
pCG616	pCG589	Gibson-saeconstr-for	ATTTAGAATAGGCGCGCCTGAATTCTTATTGTGGCAAAAGGTTTATAA ATTTTAATAC
		Gibson-saeconstr-rev	ATCCCCGGGTACCGAGCTCGAATTCTTACAAACAAAAAGCGGATTAC
pCG618	pCG599	Q5SDMpCG618F	AAGACCGCAGAGCACATAAGTAAATTTTTTTAG
		Q5SDMpCG618R	AGGGGAGTTAATAGTTGTATATATATTGAAAAAAGG
pCG620	pCG223	Gibson-saeconstr-for	ATTTAGAATAGGCGCGCCTGAATTCTTATTGTGGCAAAAGGTTTATAA ATTTTAATAC
		Gibson-saeconstr-rev	ATCCCCGGGTACCGAGCTCGAATTCTTACAAACAAAAAGCGGATTAC
RNase Y Complementation			
pCG322	RN6390	RecA-dig-for	GTCAAGGTAAGGAAAATGTT
		hybrid-Rny-delKD-rev	TGCACCTGGACGAGCTACATTTTGACCGT
		hybrid-Rny-delKD-for	ACGGTCAAAATGTAGCTCGTCCAGGTGCA
		SAV1287-rev	AACAATTTGTTGCAATTG
		BamHI-RNY-for	CCGGATCCGTTAAACTTAGCAAATATCCT
		EcoRI-RNY-rev	CGAATTCCTCAACTTAGAAATAAATCCTA
pCG596	pCG296	Q5SDMpCG296R	GCTCGTTTCGCTAATGTC
		Q5SDMpCG296F	TGGACTTTTAGCTGCTGTTGGTAAAGCAATTGATC
Race			
		RNA 5′ adapter	CTAGTACTCCGGTATTGCGGTACCCTTGTACGCCTGTTTTATA
		gfp-rev1	TCTTTTGTTTGTCTGCCAT
		Race 2	Race 2 GTATTGCGGTACCCTTGT
		gfp-rev-all	GGTATCACCTTCAAACTTGACTT
DIG probes			
gfp	pCG188	gfp-dig-for	CACTTGTCACTACTTTCGGTT
		gfp-dig-rev	TCTCTCTTTTCGTTGGGAT
saeP	RN6390	uorf4358	TATTATTTGCCTTCATTTTA
		lorf4616	ACCTTTTGATGATTTGTAGTTAG
rny	RN6390	SAV1286dig-for	TTATTAGAGAAGCAGGTGAACA
		SAV1286dig-rev	TCTTCAGGAGATACAATCACTC
rny 5 prime	RN6390	RNY-dig-for2	TTCATATAAAGAGCAAACCC
		RNY-dig-rev2	TTTTGATATTGTCAGCTTCT
rnjA	RN6390	sav1089digfor	CACCGATACCACTACCAT
		sav1089digrev	ACCTGAAGATACCGTTGT
RT-qPCR			
saeR standard	Newman	T7sae	TAATACGACTCACTATAGGGAGAAACTGCCAAAACACAAGA
		saeR2	CCATTATCGGCTCCTTTCA
saeP standard	Newman	T7-ORF4	TAATACGACTCACTATAGGGAGACAAATTGAAGAAATGAGGAGTTA
		lorf4616	ACCTTTTGATGATTTGTAGTTAG

Table 2. Continued

Purpose	Template	Name	Sequence
saeR		saeR4	TAGTCATATCCCCAAACTT
		saeU4	CCATTTACGCCTTAACTTTA
saeP		uorf4358	TATTATTTGCCTTCATTTTA
		lorf4616	ACCTTTTGATGATTTGTAGTTAG
Protein purification			
pCG249	Newman	Xho-rny-pETfor	GGGGCTCGAGCGAAATTTGTTGCTTCAAAAG
		Bam-rny-pETrev	GGGGGGATCCTTATTTCGCATATTCTACTGCT
Transcripts for RNase Y *in vitro* cleavage assay			
	pCG212 and pCG484	T7saeorf4u	TAATACGACTCACTATAGGGAGACAAATTGAAGAAATGAGGAGTTA
		LCgfpmut3.1rev1	TCTTTTGTTTGTCTGCCAT

Construction of strains complemented with RNase Y with a deletion or mutations (H367A, D368A) in its active site. A 300-bp deletion in the RNase Y active site was introduced by overlapping PCR employing oligonucleotides listed in Table 2. The amplicon was cloned into BamHI/EcoRI-digested pCG246 to generate plasmid pCG322. The H367A and D368A mutations in the RNase Y active site were introduced into plasmid pCG296 by site-directed mutagenesis (SDM Q5 Kit) according to the manufacturer's instructions (New England Biolabs) to generate plasmid pCG596. Both plasmids were cloned into *E. Coli* DC10B and then introduced into Newman *rny* mutant.

RNA isolation, northern blot hybridization and quantitative RT-qPCR

RNA isolation and northern blot analysis were performed as described previously (35). Briefly, bacteria were lysed in 1 ml of TRIzol reagent (Invitrogen) with 0.5 ml of zirconia-silica beads (0.1 mm diameter) in a high-speed homogenizer. RNA was then isolated as described by the manufacturer. For northern blot analysis, digoxigenin (DIG)-labeled DNA probes for the detection of specific transcripts were generated using a DIG-labeling PCR kit as described by the manufacturer (Roche Life Science) with the oligonucleotides listed in Table 2.

The transcript abundance of *saeR* and *saeP* from three independent experiments was determined by real-time RT-qPCR (run in duplicate) as described previously (36). Briefly, 5 μg of each RNA sample was treated with DNaseI for 30 min at RT, and the reaction was stopped with a DNase inactivation reagent (Invitrogen). RNA was then diluted 1:10, and one-step qRT-PCR was performed with the amplification kit for SYBR Green (Roche Life Science) using the appropriate oligonucleotides listed in Table 2.

For quantification, sequence-specific RNA transcripts for *saeR* and *saeP* were prepared as previously described (36). Briefly, gene-specific primers with a 5′ extension, including the T7 promoter sequence (Table 2), were used for standard PCR. T7-driven *in vitro* transcription was performed using a standard transcription assay (T7-MEGAshortscript; Invitrogen). After DNase I treatment, RNA was recovered using the MEGAclear Kit (Invitrogen), and RNA quantification was performed spectrophotometrically. Purity was verified on denaturating agarose gels and A260/280 ratio. Standard curves of sequence-specific RNA standards were generated by serial dilution (1×10^6, 3.16×10^5, 1×10^5, 3.16×10^4, 1×10^4, 3.16×10^3 and 1×10^3), and the copy numbers of the sample transcripts were calculated with the aid of light cycler 480 software (absolute quantification/2nd derivative max, Roche Life Science). Amplification of *saeP* and *saeR* occurred with an efficiency of 1.85 and 1.89 and an error of 0.012 and 0.011 respectively.

5′ Rapid amplification of cDNA ends

5′ Rapid amplification of cDNA ends (RACE) was performed as described previously (11). Briefly, total RNA was isolated and rRNA was removed using MICROBExpress (Invitrogen). A specific RNA 5′ adapter (Table 2) was then ligated to the RNA. After phenol/chloroform extraction and ethanol precipitation, the RNA was subjected to reverse transcription using oligonucleotide gfp-rev1. Nested PCR was performed using oligonucleotides Race 2 and *gfp*-rev-all (Table 2). The PCR amplicon was detected on a 3% agarose gel, eluted, cloned into pCRII-TOPO (Invitrogen) and sequenced.

Protein purification and *in vitro* assay

Protein purification. To construct the plasmid for the overproduction of RNase Y with N-terminal His-Tag, the coding sequence of the *rny* gene excluding the first 24 residues comprising a putative transmembrane domain was PCR-amplified using the primers listed in Table 2. The amplicon was ligated into XhoI/BamHI-digested pET-11b vector (Novagen), resulting in pCG249. *E. coli* BL21 (DE3) transformed with pCG249 or with an empty plasmid (as control) was grown in Luria-Bertani broth containing 100 μg ml^{-1} ampicillin and 25 μg ml^{-1} chloramphenicol at 37°C to an OD600 of 0.5. Protein expression was induced in both BL21 strains (for RNase Y expression and empty control) with 1 mM IPTG for 2 h. Bacterial cells were harvested by centrifugation and suspended in lysis buffer (100 mM NaH_2PO_4, 10 mM Tris, 8 M irea and 10 mM imidazol pH 8). EDTA-free protease inhibitor cocktail (Roche Life Science) and lysozyme (1 mg ml^{-1}) were added and the mixture was shaken at room temperature for 30 min. Complete lysis was achieved by sonication. The resulting homogenate was centrifuged at 10000 × *g* for 30 min to pellet the cellular debris. A total of 1 ml of 50% Ni-NTA slurry (Quiagen) was added to 4 ml of lysate and mixed gently by shaking for 60 min. Column purification was then performed following the manufacturer's instructions (Quiagen). The eluted fractions were analyzed by sodium dodecyl sulphate-polyacrylamide gel electrophoresis to check for

purity. The fractions containing recombinant protein were collected and dialyzed against HEPES 20 mM, NaCl 100 mM, glycerin 30%, $MgCl_2$ 1 mM and sodium deoxycholate 0.2% for 24 h at 4°C. Purification procedure was performed in parallel using BL21 with pET-11b and used as control in the activity assays.

Enzymatic activity. To monitor enzymatic activity, an assay for phosphodiesterase activity against 1 mM bis-pNpp (Roche Life Science) was used, as previously described (27). Recombinant RNase Y was added to HEPES 20 mM and NaCl 100 mM at pH 8 containing 1 mM $MnCl_2$. The chromogenic substrate bis-pNPP (*p*-nitrophenyl phosphate) was added at 1 mM. Reactions were carried out in 100 μl volumes in 96-well microtitre plates at 37°C. Hydrolysis of bis-pNPP was monitored measuring the increase in absorbance at 405 nm with the help of the Infinite 200 ProSeries Reader (Tecan).

RNase Y cleavage assay. Sequence-specific RNA transcripts for constructs pCG212 and pCG484 were prepared by *in vitro* transcription using the primers listed in Table 2. T7-driven *in vitro* transcription was performed in a standard transcription assay (T7-MEGAshortscript). After DNase I treatment, RNA was recovered using the MEGAclear Kit (Invitrogen), and RNA quantification was performed spectrophotometrically. RNase Y cleavage assay was performed using 0.125 μg of RNA substrate and purified 1.36 μM of RNase Y or control dialysate of Bl21, pET-11b cells in a reaction volume of 10 μl (20 mM HEPES pH 8, 100 mM NaCl, 1 mM $MnCl_2$ or 8 mM $MgCl_2$). The reactions were incubated for 10 min at 30°C. After ethanol precipitation, RNA was dissolved in 10 μl loading buffer (50% formamide, 6.5% formaldehyde, 3 μg ethidiumbromide, in 40 mM 3-(N-morpholino) propanesulfonic acid buffer) and RNA was loaded onto denaturating agarose gel (1% agarose, 1.8% formaldehyde in 40 mM 3-(N-morpholino) propanesulfonic acid buffer). Transcripts were detected by northern blot analysis using *gfp* DIG probes created as described above.

RESULTS

The monocistronic transcript T4 encoding *saeP* arises via termination

RNase Y is involved in the processing of the primary T1 transcript of the *sae* operon, which leads to the formation of the stable T2 RNA (11,20) encoding the response regulator SaeR and the histidine kinase SaeS (Figure 1A). This processing event occurs at a CS (11) that is flanked by two stem loops (Figure 1A). Interestingly, the upstream stem loop was previously predicted to be a *rho*-independent terminator (37). Thus, the small T4 RNA encoding *saeP* could be either a processed product of T1 or generated by premature termination of a *de novo* transcript.

To address this question and to further study the impact of the various structural elements in *sae* processing, the *saePQ* region, including the promoter P1 and carrying different deletions flanking the CS, was fused to a truncated *gfp* gene without a ribosome binding site (Figure 1B). A stop codon was introduced into the *saeP* gene to prevent any possible interference of the SaeP protein with transcription. The *sae-gfp* constructs (Figure 1B) were integrated into the wild-type strain and the *rny* mutant, in which the native *saeP* was replaced with a *kanA* resistance cassette. This procedure allowed the detection of the artificial RNAs by northern blot analysis using probes lying upstream (*saeP*) and downstream (*gfp*) of the CS without detection of the native *saePQRS* operon (Figure 1C).

In the wild-type strain carrying the reference construct pCG212, two bands were detected using both *gfp* and *saeP* probes (Figure 1C, lane 1). In both cases, the band with the higher molecular weight corresponded to the unprocessed transcript T1. The bands with lower molecular weights corresponded to T2 in the case of the *gfp* probe and to T4 in the case of the *saeP* probe. In the *rny* mutant carrying different constructs, T2 could not be detected, confirming that RNase Y is involved in the processing and generation of T2 (Figure 1C, lanes 7–12, *gfp* panel). However, T4 was also detectable in the *rny* mutant (in which no processing occurs) as long as the proposed terminator structure (the first stem loop in constructs pCG212, pCG213 and pCG218) was present (Figure 1C, lanes 7–9, *saeP* panel). In constructs lacking this stem loop (pCG219, pCG379 and pCG223), T4 was neither detectable in the wild-type nor in the mutant strain (Figure 1C, lanes 4–6 and 10–12, *sae*P panel). This indicates that T4 arose via premature termination at the *rho*-independent terminator and not from processing of the T1 transcript. Thus, the upstream fragment resulting from RNase Y cleavage is subject to rapid degradation by 3′ exonuclease activity which is not inhibited by T4 terminator structure (Figure 1C, compare lanes 1–3 with lanes 7–9). If the terminator structure was inhibiting the exonuclease activity, one would expect to see more T4 RNA (arising from the combination of transcription termination and RNase Y cleavage followed by chew back till the terminator structure) in the wild-type relative to the *rny* mutant.

Altogether the above findings suggest that, on one hand the upstream fragment resulting from RNase Y cleavage is subjected to rapid degradation. On the other, the downstream fragment (T2) is stabilized (11). Thus, RNase Y allow differential expression of the genes that are co-expressed in the *saePQRS* operon, which should be reflected by the relatively higher expression of *saeRS* compared to *saeP*. To investigate this hypothesis, we performed qRT-PCR in the Newman wild-type, the *rny* mutant and in the complemented strain with ectopic expression of RNase Y to quantify transcript abundance of *saeR* and *saeP*. P1 and P3 promoter activity in Newman are not altered by RNase Y deletion (11) and, therefore, the difference in *saeR* levels between the wild-type and the *rny* mutant are attributable solely to altered RNA processing. As shown in Figure 1D, the ratio between *saeR* and *saeP* was lower in the *rny* mutant compared with the wild-type. This effect could also be complemented by ectopic expression of RNase Y. In this strain the *saeR*/*saeS* ratio is even higher than the wild-type, in accordance with excess RNase Y by ectopic expression. Thus, RNase Y allows differential expression between genes that are co-expressed in the *saePQRS* operon, shifting the balance towards *saeRS*.

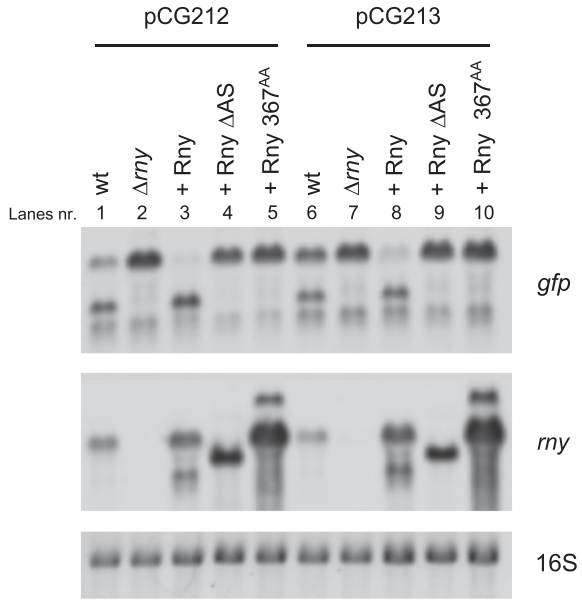

Figure 2. *sae* processing requires an active RNase Y. Wild-type, *rny* mutant, complemented strain with truncated RNase Y lacking its active site (ΔAS) and complemented strains with RNase Y with point mutations in His367 and Asp368 that constitute the highly conserved HD motif (367^{AA}), all carrying the *sae-gfp* constructs indicated in the figure, were grown to exponential phase. RNA was harvested and hybridized to DIG-labeled DNA probes specific for *gfp* or *rny*. As a loading control, 16S rRNA was detected in the ethidium bromide-stained gel, as shown at the bottom of the figure.

An active form of RNase Y is required for *sae* processing

RNase Y in *B. subtilis* is thought to act as a scaffold for the formation of a protein complex resembling the *E. coli* degradosome (9,22,23,25); the presence of a similar degradosome-like complex has also been suggested for *S. aureus* (24). Thus, it is feasible that RNase Y may not directly cleave the *sae* transcript but rather recruits other proteins responsible for this cleavage (e.g. RNase J1). To address this question, active site mutants of RNase Y were analyzed in a complementation assay. Plasmids with cloned genes coding for full-length RNase Y, truncated RNase Y lacking its active site (ΔAS) or RNase Y with point mutations in His367 and Asp368 that constitute the highly conserved HD motif (367^{AA}), were introduced into *rny* mutant strains carrying the artificial *sae-gfp* constructs pCG212 and pCG213. Processing was then analyzed by northern blot analysis using *gfp*-specific probes. Only complementation with full-length, intact RNase Y could restore cleavage (Figure 2A, lanes 3 and 8).

SaeP does not influence RNase Y-dependent processing

To further define the sequence/structural requirements for RNase Y-dependent cleavage, an additional *sae-gfp* construct carrying just the region encompassing the two stem loops but lacking *saeP* was designed (pCG301) (Figure 3A). The construct was integrated into the chromosome of Newman wild-type and *rny* mutant strains, and processing was analyzed by northern blot analysis using a *gfp*-specific probe (Figure 3B). RNase Y-dependent processing was still detectable. Thus, upstream sequences lying within the co-transcribed *saeP* gene are dispensable for RNase Y activity.

The results shown in Figure 1 were obtained in a strain in which *saeP* was deleted. In order to rule out any possible interference of SaeP deletion with our previous conclusions, the *sae-gfp* constructs were also analyzed in Newman wild-type background, providing essentially the same results (compare Figures 1C and 3C): in the wild-type strains, processing was indicated by two bands, whereas only the unprocessed transcript was detectable in the *rny* mutant. Only a large deletion encompassing the CS (construct pCG223) prevented cleavage.

RNase Y cleavage is not determined by the CS sequence

Interestingly, the deletion of 13 bp encompassing the cleavage site (construct pCG213) did not prevent cleavage by RNase Y (Figures 1C and 3C). Next, we mapped the cleavage site in construct pCG213 by 5′ RACE (Figure 3D). Sequencing of various clones revealed the cleavage sites all mapped to the same position, allowing the detection of what we called an 'alternative cleavage site (aCS)'. The aCS mapped precisely 13 nt upstream of the native CS (11). Interestingly, the deletion in construct pCG213 was also 13 nt long, suggesting that RNase Y may recognize a specific sequence/structure downstream of CS and cleave at a specific distance.

To further investigate this hypothesis, two additional constructs were designed (Figure 4A). Construct pCG392 carries a 24-bp deletion downstream of CS, whereas construct pCG394 carries a deletion of both CS and aCS. These two constructs were integrated into the chromosome of Newman wild-type and *rny* mutant strains and analyzed by northern blot analysis using a *gfp*-specific probe. The reference construct pCG212 was included in the analysis as a control.

Cleavage still occurred in construct pCG394, and a band corresponding to the processed RNA was indeed visible in the wild-type strain (indicated in the image by an asterisk). To further investigate this cleavage, we performed 5′ RACE analysis. Various clones were sequenced and all mapped to the same position (Figure 4C), allowing the detection of another alterative cleavage site (aCS2) exactly 20 nt upstream of the standard CS. The deletion in construct pCG394 was also 20 nt long.

Double strand structure downstream of CS

In construct pCG392 (carrying a 24-bp deletion downstream of CS), cleavage no longer occurred (Figure 4B), indicating that RNase Y requires a sequence or structure (underlined in Figure 4D, tentatively named 'RNase Y recognition sequence, Rrs') located downstream of CS to cleave at a specific distance upstream. To gain further insights into RNase Y requirements, the secondary structure of the region downstream of CS was predicted using mfold software (38). We found that in all constructs in which processing could still occur (i.e. pCG212, pCG213, Figure 5 or pCG218, pCG219 and pCG379, Supplementary Figure S1), the Rrs formed a double-strand structure with a specific sequence that we termed 'Rrs counterpart'. This double-

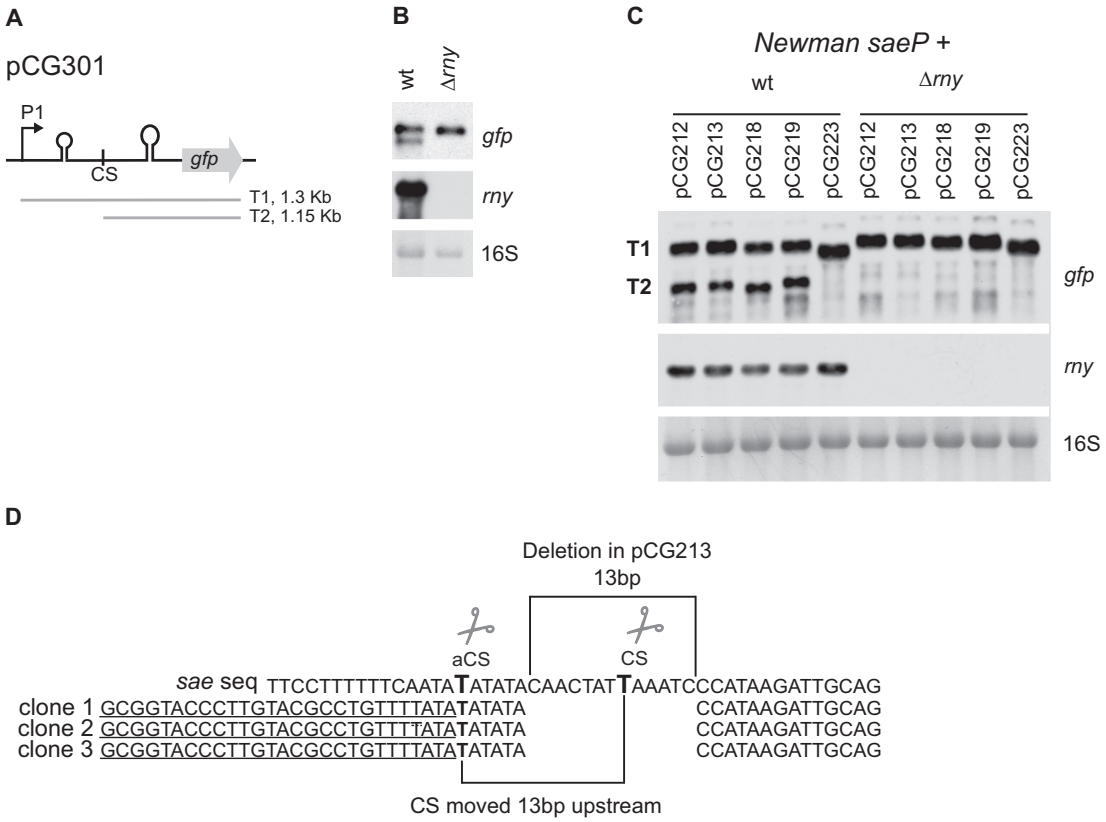

Figure 3. RNase Y-dependent cleavage is independent from *saeP* and CS sequences. (**A**) Schematic representation of construct pCG301 carrying just the region of *sae* between the two stem loops under the native promoter P1. Below the construct, the RNAs observed in the northern blot analysis are indicated. (**B**) Northern blot analyses to examine *sae* processing of the pCG301 construct. Newman wild-type and *rny* mutant strains carrying pCG301 were grown to the exponential phase, and RNA was harvested and hybridized to a DIG-labeled DNA probe specific for *gfp* and *rny*. The 16S rRNA detected in ethidium bromide-stained gel served as a loading control and is shown at the bottom of the panel. (**C**) Northern blot analyses to examine *sae* processing in strains carrying the *sae-gfp* constructs shown in Figure 1B. Newman wild-type and *rny* mutant strains carrying the different constructs were grown to exponential phase. RNA was then harvested and hybridized to DIG-labeled DNA probes specific for *gfp*, *saeP* and *rny*. As a loading control, 16S rRNA was detected in ethidium bromide-stained gel, as shown at the bottom of the panel. (**D**) Mapping of the 5′ end of the processed RNA in construct pCG213 by RACE analyses. cDNA was obtained using RNA from the Newman wild-type strain carrying pCG213. The *sae* sequence shown in the panel is aligned with those of three different clones (1, 2 and 3). The RNA 5′ adapter is underlined, and the mapped position for the alternative cleavage site (aCS) is indicated in bold. The deletion in construct pCG213 and the shift of the CS are also shown.

stranded structure was not predicted in constructs with impaired processing (i.e. pCG392, Figure 5), supporting the possibility that this is the structure recognized by RNase Y.

To confirm the importance of the double-strand structure consisting of the Rrs and the Rrs counterpart, we analyzed a new construct (pCG484) carrying a deletion of this Rrs counterpart (Figure 6A and Supplementary Figure S1). As observed in Figure 6B, in the wild-type strain carrying pCG484 only one band was visible, which corresponded to the unprocessed transcript. This result indicated that the Rrs counterpart also is necessary for cleavage.

Next, we created construct pCG618 carrying single point mutations that prevent formation of the proposed double-strand structure (Figure 6C and Supplementary Figure S1). This construct was cloned into a replicative vector. As a control, we cloned our reference construct pCG212 (which is an integrative vector) into the same replicative vector, yielding construct pCG599. Both constructs were then transformed into the Newman strain and processing was analyzed by northern blot analysis using a *gfp*-specific probe. As can been seen in Figure 6D, cleavage was detectable in construct pCG599 but not in construct pCG618, thus further indicating that disturbing the secondary structure hinders cleavage.

So far, we have shown that cleavage does not depend on a distinct cleavage signature. However, all three determined cleavage sites (CS, aCS1 and aCS2) are characterized by a conserved T. To analyze whether this T is required for cleavage, we substituted it for a C in construct pCG616 (Figure 6C) and transformed this into the Newman wild-type strain. As can been seen in Figure 6D, the exchange did not prevent cleavage, thus corroborating the hypothesis that RNase Y cleavage is not dependent on a distinct cleavage signature.

Role of RNase J1 for *sae* stabilization/processing

Cleavage of the *sae* transcript by RNase Y leads to stabilization of the generated downstream product (11). Thus, it could be hypothesized that the predicted secondary structure, instead of being a recognition site for RNase Y, is involved in protection of the downstream fragment from degradation by RNase J1/J2. In this case, RNA transcripts

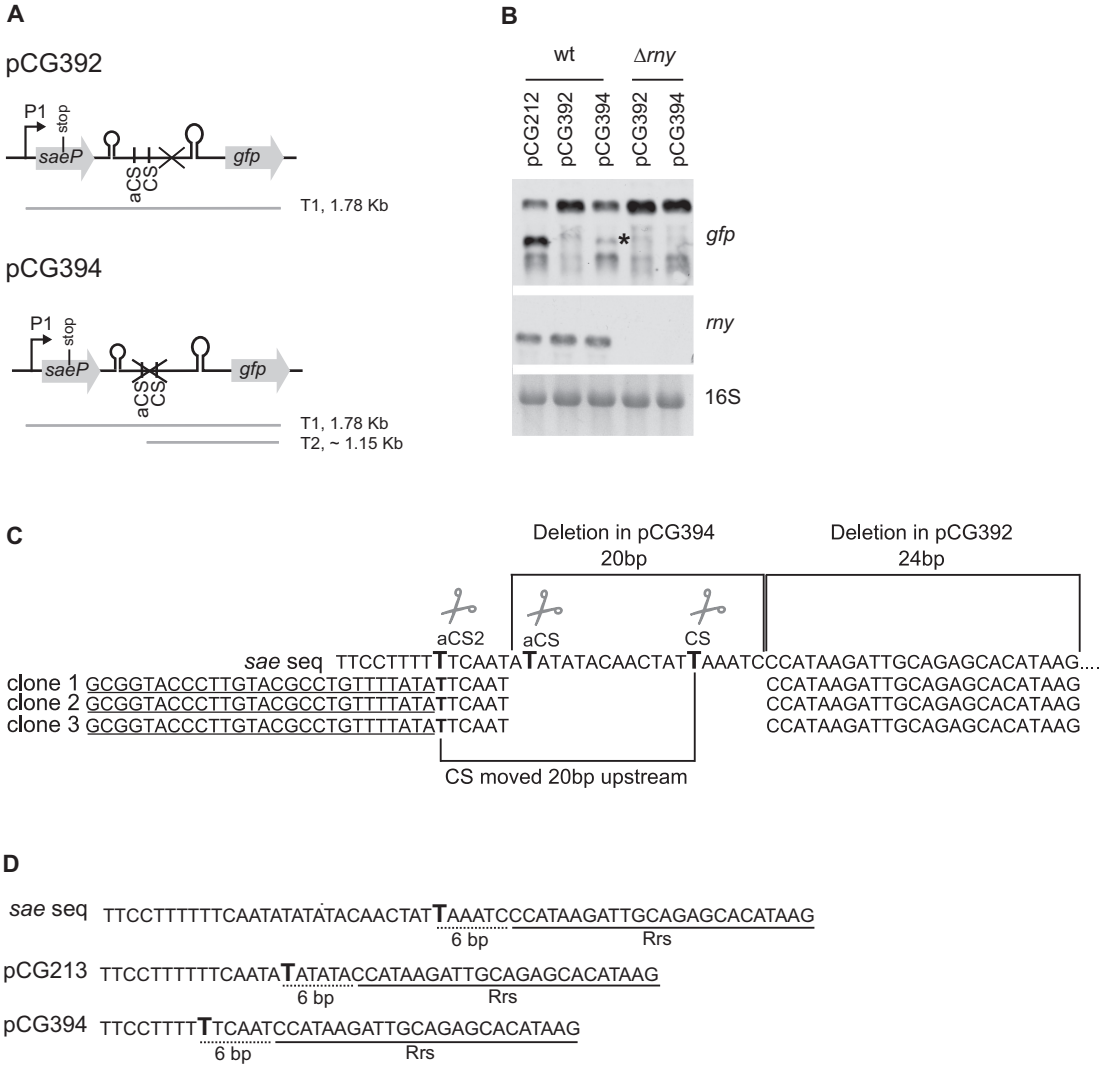

Figure 4. RNase Y-dependent cleavage occurs 6 nt upstream of putative recognition determinant. (**A**) Schematic representation of constructs pCG392 and pCG394 carrying a deletion downstream of CS and a deletion of both aCS and CS, respectively (deletions are indicated in the panel as a cross). The RNAs detected in the northern blot analysis are shown below each construct. (**B**) Northern blot analyses to examine *sae* processing in strains carrying pCG392 and pCG394. Newman wild-type and *rny* mutant strains carrying the different constructs were grown to exponential phase (Newman pCG212 was included in the analysis as a control). RNA was then harvested and hybridized to DIG-labeled DNA probes specific for *gfp* and *rny*. As a loading control, 16S rRNA was detected in the ethidium bromide-stained gel, as shown at the bottom of the panel. The processed RNA found in construct pCG394 is indicated by *. (**C**) Mapping of the 5′ end of the processed RNA in construct pCG394. The *sae* sequence is aligned with those of three different clones (1, 2 and 3). The RNA 5′ adapter is underlined, and the mapped position for alternative cleavage site 2 (aCS2) is shown in bold. The deletion in construct pCG394 and the shift in the CS are also indicated. (**D**) The RNase Y recognition sequence (Rrs) is underlined; the distance between Rrs and the cleavage sites (CS, aCS or aCS2) is underlined with dots.

arising from constructs in which the formation of this structure is hindered (i.e. pCG392 and pCG484) might be unprotected, and not accumulate sufficiently to be detected by our assay. To address this question, we analyzed *sae-gfp* processing in the recently described *rnjA* mutant of strain PR01 (39). In this strain background the plasmids used so far could not be integrated via transduction or transformation. Therefore, we subcloned the constructs into the replicative vector pCG246.

In PR01 wild-type strain containing the replicative reporter constructs *sae-gfp* processing was similar to strain Newman harboring the integrative constructs: no cleavage was detectable in constructs missing the Rrs (pCG601), the Rrs counterpart (pCG600) or the whole region (pCG620). Surprisingly, in the *rnjA* mutant of PR01, processed fragments were detectable in all constructs. These results would suggest that the secondary structure may have a protective function in avoiding degradation by RNase J1. However, processing could also be detected in construct pCG620 (equivalent to pCG223), in which the whole region encompassing the CS is missing. These results suggest that without RNase J1, the activity of RNase Y is somehow altered, leading to so far unobserved processing events.

Of note, while carrying out our usual controls with the *rny* probe, we found that *rnjA* deletion resulted in an alter-

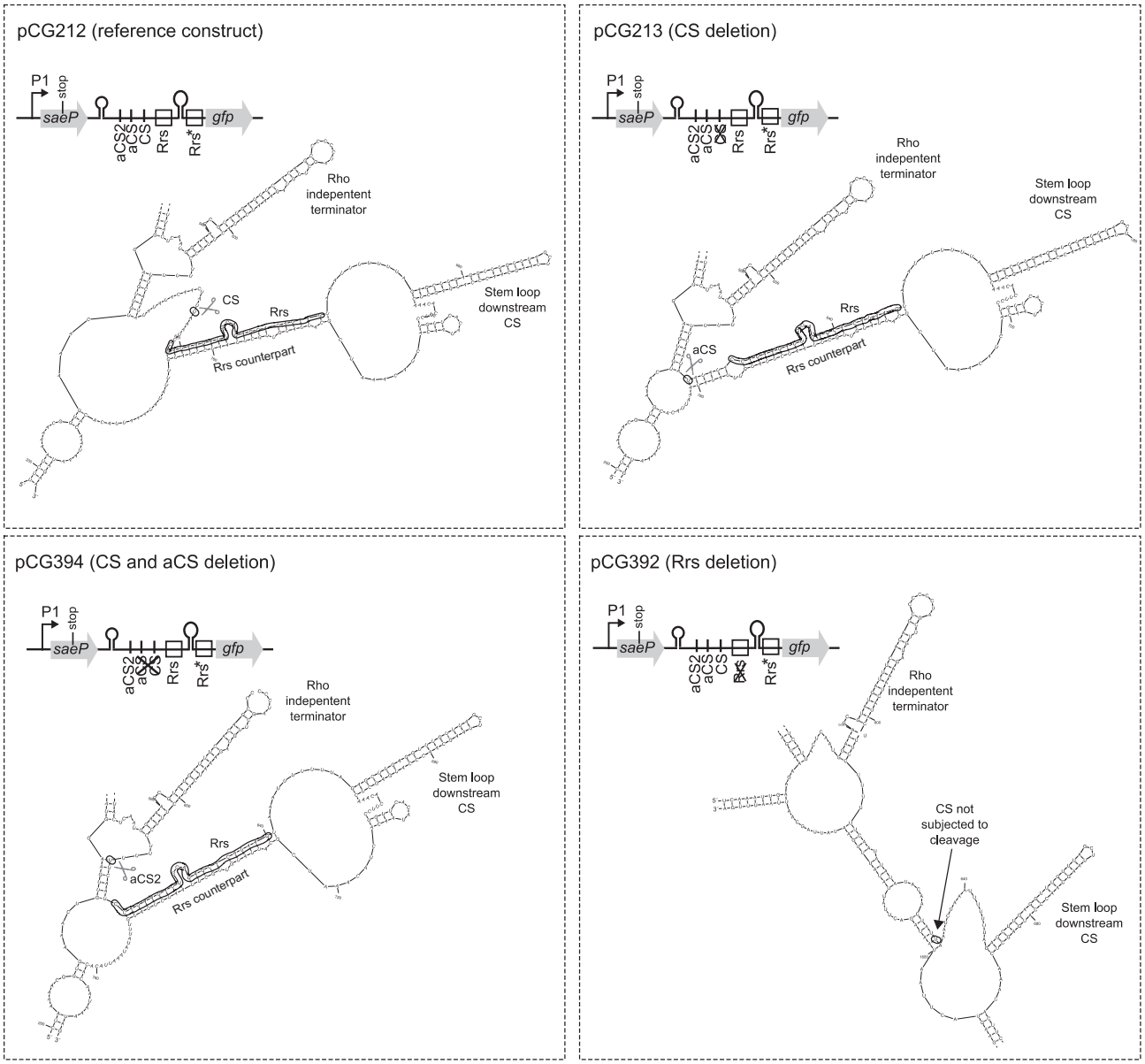

Figure 5. Secondary structure downstream of CS. Prediction of secondary structures of *sae*-fragments cloned in pCG212, pCG213, pCG394, pCG392 and pCG408 by the mfold software (38). In each panel, the schematic representation of the construct is shown together with the predicted secondary structure (CS: cleavage site; aCS1: alternative cleavage site1; aCS2: alternative cleavage site 2; Rrs: RNase Y recognition sequence; Rrs*: Rrs counterpart). Deletions are indicated by a cross. In the predicted secondary structure, when present, Rrs is encircled with a bold line. For clarity, only the portion of the transcript that is of interest is shown.

ation of the *rny* transcript, with the appearance of a highly abundant smaller transcript (Figure 7B, panel *rny*).

We next analyzed the PR strains (without any constructs) and compared them to the Newman strains by northern blot analysis (Figure 7C). Again, in the *rnjA* mutant, a highly abundant smaller transcript of *rny* was detectable. With the use of a *rny* probe covering the 5′ end of the *rny* transcript, this smaller transcript was no longer detectable (Figure 7C panel *rny* 5′), indicating that the smaller *rny* transcript accumulating in the *rnjA* mutant is missing the 5′ end. A putative internal start codon and ribosomal binding site can be predicted within this truncated *rny* fragment. Thus, the fragment may encode an N-terminal truncated RNase Y with altered requirements and activity. This assumption is supported by our finding that expression of RNase Y without the N-terminal membrane anchor was not possible in *S. aureus.* Interestingly, purified anchorless RNase Y was shown to elicit high RNA degrading activity toward *in vitro* transcribed *sae-gfp*-RNA with no cleavage specificity (Supplementary Figure S2). However, the interpretation of this data is hindered by some experimental limits, e.g. the molecular ratio of RNase Y versus substrate or other experimental conditions might be highly important for maintaining the specificity. We also cannot rule out that RNA degradation is a least partially due to RNases from *E. coli* which co-purify with RNase Y.

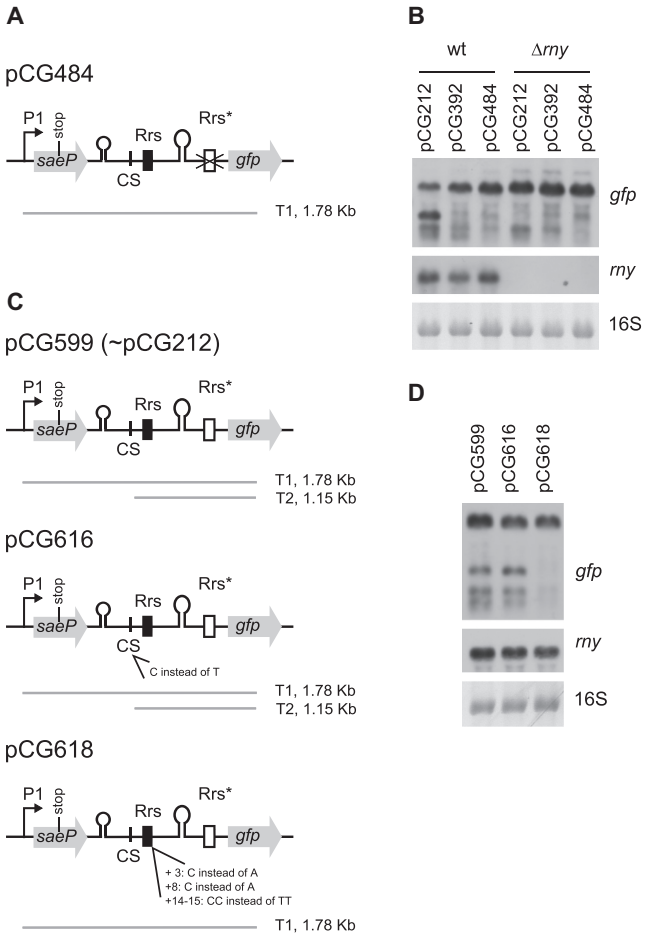

Figure 6. Double strand structure downstream of CS determines *sae* processing. (**A**) Schematic representation of construct pCG484 carrying a deletion in the Rrs counterpart (Rrs*, indicated by a white rectangle). The RNAs detected in the northern blot analysis are shown below each construct. (**B**) Northern blot analyses to examine *sae* processing in strains carrying pCG384. Newman wild-type and *rny* mutant strains carrying the different constructs were grown to the exponential phase (strains carrying pCG212 and pCG392 were included in the analysis as controls). RNA was harvested and hybridized to DIG-labeled DNA probes specific for *gfp* and *rny*. As a loading control, 16S rRNA was detected in the ethidium bromide-stained gel, as shown at the bottom of the panel. (**C**) Schematic representation of construct pCG599 (reference construct in replicative vector, equivalent to pCG212), pCG616 (carrying point mutation in CS) and pCG618 (carrying point mutations which affect Rrs secondary structure). The RNAs detected in the northern blot analysis are shown below each construct. (**D**) Northern blot analyses to examine *sae* processing in strains carrying pCG599, pCG616 und pCG618. Newman wild-type carrying the different constructs was grown to exponential phase. RNA was harvested and hybridized to DIG-labeled DNA probes specific for *gfp* and *rny*. As a loading control, 16S rRNA was detected in the ethidium bromide-stained gel, as shown at the bottom of the panel.

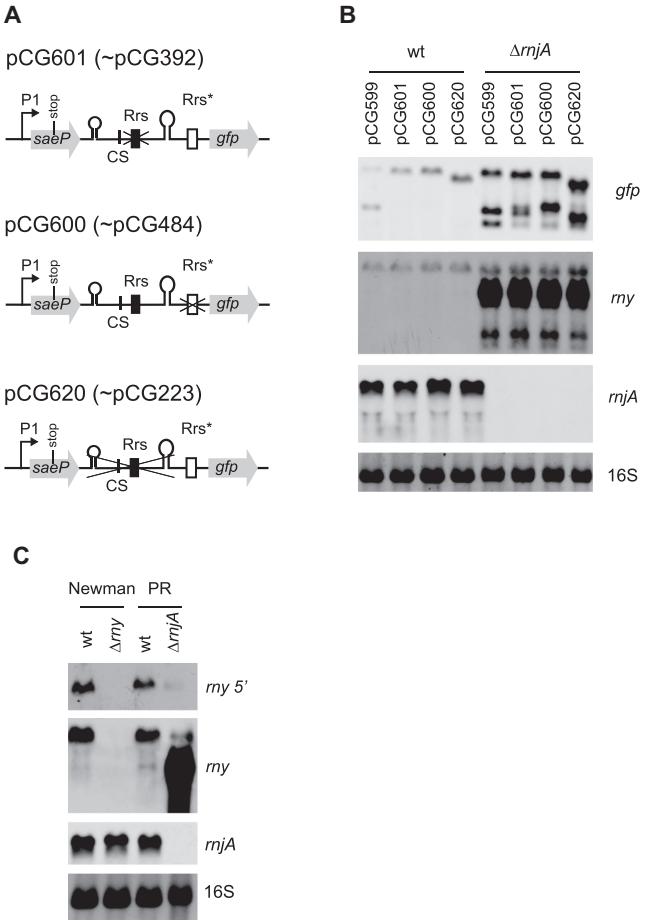

Figure 7. Interference of RNase J1 with RNase Y activity. (**A**) Schematic representation of construct pCG601, pCG600 and pCG620, which are the equivalent in replicative plasmid of construct pCG392, pCG484 and pCG223, respectively. (**B**) Northern blot analyses to examine *sae* processing in strains carrying pCG600, pCG601 and pCG620. PR wild-type and *rnjA* mutant strains carrying the different construct were grown to the exponential phase (strains carrying the reference construct pCG599 were included in the analysis as controls). RNA was then harvested and hybridized to DIG-labeled DNA probes specific for *gfp*, *rny* and *rnjA*. As a loading control, 16S rRNA was detected in the ethidium bromide-stained gel, as shown at the bottom of the panel. (**C**) Northern blot analyses to detect *rny* transcript in PR strains. Newman wild-type and *rny* mutant, PR wild-type and *rnjA* mutant strains were grown to exponential phase. RNA was harvested and hybridized to DIG-labeled DNA probes specific for *rnjA*, *rny* and *rny* 5′. As a loading control, 16S rRNA was detected in the ethidium bromide-stained gel, as shown at the bottom of the panel.

DISCUSSION

RNase Y allows differential expression of genes that are co-transcribed in the same operon

SaeR and SaeS are part of a bacterial two-component system with a response regulator and a histidine kinase that control the expression of major virulence genes in *S. aureus* (14–16). These two proteins are co-transcribed in the *saePQRS* operon with two additional proteins (SaeP and SaeQ). A total of four overlapping RNAs are transcribed, with the major and more stable transcript being generated by endonucleolytic cleavage of the full length T1 transcript by RNase Y (11,20). We show that the monocistronic transcript encoding *saeP* is a *de novo* transcript from P1 that ends at the *rho*-independent terminator and does not arise from processing of the full length transcript (Figure 1). RNase Y cleavage of the full length T1 transcript leads, on the one hand, to stabilization of the downstream fragment and, on the other, to destabilization of the upstream fragment. Thus, RNase Y allows differential expression between the genes that are co-expressed in the *saePQRS* operon, shifting the balance towards *saeRS* (as confirmed

by qRT-PCR, Figure 1D). SaeP and SaeQ are important to return the activated *sae* system to its pre-stimulated state (17,19). Thus, RNase Y cleavage might be important in response to certain stress conditions to modulate activation of the *sae* system to limit *saeP* expression in favor of *saeRS*.

In *B. subtilis*, the current model of RNA decay entails endonucleolytic cleavage by RNase Y followed by 5′-3′ exonucleolytic degradation by RNase J1 and PNPase 3′-5′ exonucleolytic activity (10,29,30). The importance of RNase Y processing in operon regulation has also been described in *B. subtilis* for the polycistronic *infC-rpmI-rlpT* (40) and the *gapA* operons (22). Nevertheless, RNase Y cleavage in the *infC-rpmI-rlpT* operon is needed for subsequent 5′-3′ exonucleolytic degradation of the processed RNA by RNase J1 (40). This phenomenon differs from the action of RNase Y in the *sae* operon, where the downstream transcript arising from cleavage (T2) is stabilized. This may be a special feature of the *sae* operon, in which the downstream fragment is potentially protected, *e.g.* via RNA secondary structures and/or binding proteins. Stabilization of RNase Y-derived cleavage products has also been observed in other species. In *Streptococcus pyogenes*, RNase Y cleaves a longer *speB* transcript, leading to a shorter, more stable transcript (41). Recently, *Clostridium perfringens* RNase Y has also been shown to be involved in post-transcriptional stabilization of virulence genes *colA* and *pilA* (42). Thus, stabilization of RNase Y cleavage products may be more common than previously recognized.

The RNase Y-generated *sae* upstream transcript seems to be rapidly degraded via a 3′-5′ exonuclease, presumably PNPase. To compensate for the rapid degradation of *saeP* upon RNase Y cleavage, an internal transcription terminator upstream of the CS ensures the expression of *saeP*.

Role of secondary structure downstream of cleavage site

Secondary structure prediction revealed that RNase Y is likely to recognize a double-stranded RNA region that forms between Rrs and its counterpart. Moreover, mutations within Rrs and deletion of the Rrs counterpart also inhibited cleavage. These results indicate that the specificity for cleavage is determined by a downstream secondary structure. Khemici *et al.* (12) also suggested that adjacent secondary structures are probably crucial for RNase Y specificity as bioinformatics analyses of 99 RNase Y target genes did not reveal any common motif. In *B. subtilis*, RNase Y was shown to cleave within an AU-rich region upstream of a stem loop (8). Although the authors did not perform a detailed investigation of the deletion that would affect cleavage and, consequently, the part of the sequence that was in fact recognized by RNase Y, the secondary structure identified in their study clearly resembles the structure we describe for *sae*. It would be interesting to delete the cleavage site identified by the authors in the *yitY* leader (8) to confirm our hypothesis that RNase Y recognizes a structure downstream of the site that is then cleaved.

The elucidated secondary structure may also be involved in protection and RNA fragments stabilization. Indeed, in the strain lacking RNase J1, processed transcripts were detected, indicating that the structure protects against RNase J1. However, in the RNase J1 mutant, RNase Y activity presumably is altered, hampering the final interpretation of the results.

RNase Y cleavage is not determined by the cleavage site

Deletion of 13 nt encompassing the cleavage site of the *sae* operon did not prevent cleavage (Figures 1C and 3C). Alternative cleavage sites were detectable 6 nt upstream of a proposed recognition site (Figure 4D). Interestingly, the endonucleolytic activity of RNase E also requires the recognition of a region that is adjacent to, but not contiguous with, a segment in which cleavage can occur (43,44). RNase E favors binding to unpaired neighboring regions, whereas RNase Y appears to prefer the double-stranded sequence.

In both cases, cleavage occurs within a single-stranded stretch. RNase Y cleavage also seems to occur via a ruler-and-cut mechanism. Such a mechanism was recently elucidated for *Salmonella* RNase E enzyme (45). However, our results indicate that RNase Y in *S. aureus* may use a longer ruler of probably 6 nt. The lack of any structural data for RNase Y means that the molecular mechanism remains unsolved.

SUPPLEMENTARY DATA

Supplementary Data are available at NAR Online.

ACKNOWLEDGEMENTS

We are grateful to Peter Redder for providing the *rnjA* mutant. We would like to thank Pascale Romby and Isabelle Calderali for helpful discussions. Special thanks to Vittoria Bisanzio, Natalya Korn and Isabell Samp for excellent technical assistance.

FUNDING

'Deutsche Forschungsgemeinschaft' [Wo578/7-1]; Transregio34 [Project B1]. We acknowledge support by Deutsche Forschungsgemeinschaft and Open Access Publishing Fund of University of Tübingen.
Conflict of interest statement. None declared.

REFERENCES

1. Condon,C. and Bechhofer,D.H. (2011) Regulated RNA stability in the gram positives. *Curr. Opin. Microbiol.*, **14**, 148–154.
2. Laalami,S. and Putzer,H. (2011) mRNA degradation and maturation in prokaryotes: the global players. *Biomol. Concepts*, **2**, 491–506.
3. Lehnik-Habrink,M., Lewis,R.J., Mäder,U. and Stülke,J. (2012) RNA degradation in *Bacillus subtilis*: an interplay of essential endo- and exoribonucleases. *Mol. Microbiol.*, **84**, 1005–1017.
4. Hui,M.P., Foley,P.L. and Belasco,J.G. (2014) Messenger RNA degradation in bacterial cells. *Annu. Rev. Genet.*, **48**, 537–559.
5. Durand,S., Tomasini,A., Braun,F., Condon,C. and Romby,P. (2015) sRNA and mRNA turnover in Gram-positive bacteria. *FEMS Microbiol. Rev.*, **39**, 316–330.
6. Bonnin,R.A. and Bouloc,P. (2015) RNA degradation in *Staphylococcus aureus*: Diversity of Ribonucleases and their impact. *Int. J. Genomics*, **2015**, 1–12.
7. Richards,J., Liu,Q., Pellegrini,O., Celesnik,H., Yao,S., Bechhofer,D.H., Condon,C. and Belasco,J.G. (2011) An RNA pyrophosphohydrolase triggers 5′-exonucleolytic degradation of mRNA in *Bacillus subtilis*. *Mol. Cell*, **43**, 940–949.

8. Shahbabian,K., Jamalli,A., Zig,L. and Putzer,H. (2009) RNase Y, a novel endoribonuclease, initiates riboswitch turnover in *Bacillus subtilis*. *EMBO J.*, **28**, 3523–3533.
9. Lehnik-Habrink,M., Newman,J., Rothe,F.M., Solovyova,A.S., Rodrigues,C., Herzberg,C., Commichau,F.M., Lewis,R.J. and Stülke,J. (2011) RNase Y in *Bacillus subtilis*: a Natively disordered protein that is the functional equivalent of RNase E from *Escherichia coli*. *J. Bacteriol.*, **193**, 5431–5441.
10. Durand,S., Gilet,L., Bessières,P., Nicolas,P. and Condon,C. (2012) Three essential ribonucleases-RNase Y, J1, and III-control the abundance of a majority of *Bacillus subtilis* mRNAs. *PLoS Genet.*, **8**, e1002520.
11. Marincola,G., Schäfer,T., Behler,J., Bernhardt,J., Ohlsen,K., Goerke,C. and Wolz,C. (2012) RNase Y of *Staphylococcus aureus* and its role in the activation of virulence genes. *Mol. Microbiol.*, **85**, 817–832.
12. Khemici,V., Prados,J., Linder,P. and Redder,P. (2015) Decay-initiating endoribonucleolytic cleavage by RNase Y is kept under tight control via sequence preference and sub-cellular localisation. *PLoS Genet.*, **11**, e1005577.
13. Kaito,C., Kurokawa,K., Matsumoto,Y., Terao,Y., Kawabata,S., Hamada,S. and Sekimizu,K. (2005) Silkworm pathogenic bacteria infection model for identification of novel virulence genes. *Mol. Microbiol.*, **56**, 934–944.
14. Steinhuber,A., Goerke,C., Bayer,M.G., Döring,G. and Wolz,C. (2003) Molecular architecture of the regulatory locus sae of *Staphylococcus aureus* and its impact on expression of virulence factors. *J. Bacteriol.*, **185**, 6278–6286.
15. Rogasch,K., Rühmling,V., Pané-Farré,J., Höper,D., Weinberg,C., Fuchs,S., Schmudde,M., Bröker,B.M., Wolz,C., Hecker,M. *et al.* (2006) Influence of the two-component system SaeRS on global gene expression in two different *Staphylococcus aureus* strains. *J. Bacteriol.*, **188**, 7742–7758.
16. Nygaard,T.K., Pallister,K.B., Ruzevich,P., Griffith,S., Vuong,C. and Voyich,J.M. (2010) SaeR binds a consensus sequence within virulence gene promoters to advance USA300 pathogenesis. *J. Infect. Dis.*, **201**, 241–254.
17. Jeong,D.-W., Cho,H., Lee,H., Li,C., Garza,J., Fried,M. and Bae,T. (2011) Identification of the P3 promoter and distinct roles of the two promoters of the SaeRS Two-Component System in *Staphylococcus aureus*. *J. Bacteriol.*, **193**, 4672–4684.
18. Cho,H., Jeong,D.-W., Li,C. and Bae,T. (2012) Organizational requirements of the SaeR binding sites for a functional P1 promoter of the sae operon in *Staphylococcus aureus*. *J. Bacteriol.*, **194**, 2865–2876.
19. Jeong,D.-W., Cho,H., Jones,M.B., Shatzkes,K., Sun,F., Ji,Q., Liu,Q., Peterson,S.N., He,C. and Bae,T. (2012) The auxiliary protein complex SaePQ activates the phosphatase activity of sensor kinase SaeS in the SaeRS two-component system of *Staphylococcus aureus*. *Mol. Microbiol.*, **86**, 331–348.
20. Geiger,T., Goerke,C., Mainiero,M., Kraus,D. and Wolz,C. (2008) The virulence regulator Sae of *Staphylococcus aureus*: promoter activities and response to phagocytosis-related signals. *J. Bacteriol.*, **190**, 3419–3428.
21. Adhikari,R.P. and Novick,R.P. (2008) Regulatory organization of the staphylococcal *sae* locus. *Microbiology*, **154**, 949–959.
22. Commichau,F.M., Rothe,F.M., Herzberg,C., Wagner,E., Hellwig,D., Lehnik-Habrink,M., Hammer,E., Völker,U. and Stülke,J. (2009) Novel activities of glycolytic enzymes in *Bacillus subtilis*: interactions with essential proteins involved in mRNA processing. *Mol. Cell. Proteomics*, **8**, 1350–1360.
23. Lehnik-Habrink,M., Pförtner,H., Rempeters,L., Pietack,N., Herzberg,C. and Stülke,J. (2010) The RNA degradosome in *Bacillus subtilis*: identification of CshA as the major RNA helicase in the multiprotein complex. *Mol. Microbiol.*, **77**, 958–971.
24. Roux,C.M., DeMuth,J.P. and Dunman,P.M. (2011) Characterization of components of the *Staphylococcus aureus* mRNA degradosome holoenzyme-like complex. *J. Bacteriol.*, **193**, 5520–5526.
25. Redder,P. (2016) How does sub-cellular localization affect the fate of bacterial mRNA? *Curr. Genet.*, **62**, 687–690.
26. Linder,P., Lemeille,S. and Redder,P. (2014) Transcriptome-wide analyses of 5′-ends in RNase J mutants of a gram-positive pathogen reveal a role in RNA maturation, regulation and degradation. *PLoS Genet.*, **10**, e1004207.
27. Nagata,M., Kaito,C. and Sekimizu,K. (2008) Phosphodiesterase activity of CvfA is required for virulence in *Staphylococcus aureus*. *J. Biol. Chem.*, **283**, 2176–2184.
28. Numata,S., Nagata,M., Mao,H., Sekimizu,K. and Kaito,C. (2014) CvfA protein and polynucleotide phosphorylase act in an opposing manner to regulate *Staphylococcus aureus* virulence. *J. Biol. Chem.*, **289**, 8420–8431.
29. Yao,S., Richards,J., Belasco,J.G. and Bechhofer,D.H. (2011) Decay of a model mRNA in *Bacillus subtilis* by a combination of RNase J1 5′ exonuclease and RNase Y endonuclease activities. *J. Bacteriol.*, **193**, 6384–6386.
30. Yao,S. and Bechhofer,D.H. (2010) Initiation of decay of *Bacillus subtilis rpsO* mRNA by endoribonuclease RNase Y. *J. Bacteriol.*, **192**, 3279–3286.
31. Novick,R.P. (1991) Genetic systems in staphylococci. *Methods Enzymol.*, **204**, 587–636.
32. Brückner,R. (1997) Gene replacement in *Staphylococcus carnosus* and *Staphylococcus xylosus*. *FEMS Microbiol. Lett.*, **151**, 1–8.
33. Arnaud,M., Chastanet,A. and Débarbouillé,M. (2004) New vector for efficient allelic replacement in naturally non transformable, low-GC-content, gram-positive bacteria. *Appl. Environ. Microbiol.*, **70**, 6887–6891.
34. Lee,C.Y., Buranen,S.L. and Ye,Z.H. (1991) Construction of single-copy integration vectors for *Staphylococcus aureus*. *Gene*, **103**, 101–105.
35. Goerke,C., Campana,S., Bayer,M.G., Döring,G., Botzenhart,K. and Wolz,C. (2000) Direct quantitative transcript analysis of the agr regulon of *Staphylococcus aureus* during human infection in comparison to the expression profile in vitro. *Infect. Immun.*, **68**, 1304–1311.
36. Burian,M., Rautenberg,M., Kohler,T., Fritz,M., Krismer,B., Unger,C., Hoffmann,W.H., Peschel,A., Wolz,C. and Goerke,C. (2010) Temporal expression of adhesion factors and activity of global regulators during establishment of *Staphylococcus aureus* nasal colonization. *J. Infect. Dis.*, **201**, 1414–1421.
37. de Hoon,M.J.L., Makita,Y., Nakai,K. and Miyano,S. (2005) Prediction of transcriptional terminators in *Bacillus subtilis* and related species. *PLoS Comput. Biol.*, **1**, e25.
38. Zuker,M. (2003) Mfold web server for nucleic acid folding and hybridization prediction. *Nucleic Acids Res.*, **31**, 3406–3415.
39. Redder,P. and Linder,P. (2012) New range of vectors with a stringent 5-fluoroorotic acid-based counterselection system for generating mutants by allelic replacement in *Staphylococcus aureus*. *Appl. Environ. Microbiol.*, **78**, 3846–3854.
40. Bruscella,P., Shahbabian,K., Laalami,S. and Putzer,H. (2011) RNase Y is responsible for uncoupling the expression of translation factor IF3 from that of the ribosomal proteins L35 and L20 in *Bacillus subtilis*. *Mol. Microbiol.*, **81**, 1526–1541.
41. Chen,Z., Itzek,A., Malke,H., Ferretti,J.J. and Kreth,J. (2012) Dynamics of *speB* mRNA transcripts in *Streptococcus pyogenes*. *J. Bacteriol.*, **194**, 1417–1426.
42. Obana,N., Nakamura,K. and Nomura,N. (2017) Role of RNase Y in *Clostridium perfringens* mRNA decay and processing. *J. Bacteriol.*, **199**,e00703–e00716.
43. Kime,L., Clarke,J.E., Romero,A.D., Grasby,J.A. and McDowall,K.J. (2014) Adjacent single-stranded regions mediate processing of tRNA precursors by RNase E direct entry. *Nucleic Acids Res.*, **42**, 4577–4589.
44. Clarke,J.E., Kime,L., Romero,A.D. and McDowall,K.J. (2014) Direct entry by RNase E is a major pathway for the degradation and processing of RNA in *Escherichia coli*. *Nucleic Acids Res.*, **42**, 11733–11751.
45. Chao,Y., Li,L., Girodat,D., Förstner,K.U., Said,N., Corcoran,C., Śmiga,M., Papenfort,K., Reinhardt,R., Wieden,H. *et al.* (2017) In vivo cleavage map illuminates the central role of RNase E in coding and non-coding RNA pathways. *Mol. Cell*, **65**, 39–51.
46. Monk,I.R., Shah,I.M., Xu,M., Tan,M.-W. and Foster,T.J. (2012) Transforming the untransformable: application of direct transformation to manipulate genetically *Staphylococcus aureus* and Staphylococcus epidermidis. *Mbio*, **3**, e00277–e00311.
47. Pattee,P.A. (1981) Distribution of Tn551 insertion sites responsible for auxotrophy on the *Staphylococcus aureus* chromosome. *J. Bacteriol.*, **145**, 479–488.

48. Kreiswirth,B.N., Löfdahl,S., Betley,M.J., O'Reilly,M., Schlievert,P.M., Bergdoll,M.S. and Novick,R.P. (1983) The toxic shock syndrome exotoxin structural gene is not detectably transmitted by a prophage. *Nature*, **305**, 709–712.
49. Duthie,E.S. and Lorenz,L.L. (1952) Staphylococcal coagulase; mode of action and antigenicity. *J. Gen. Microbiol.*, **6**, 95–107.
50. Helle,L., Kull,M., Mayer,S., Marincola,G., Zelder,M.-E., Goerke,C., Wolz,C. and Bertram,R. (2011) Vectors for improved Tet repressor-dependent gradual gene induction or silencing in *Staphylococcus aureus*. *Microbiology*, **157**, 3314–3323.